Amirkabir Journal of Mechanical Engineering

Amirkabir J. Mech. Eng., 52(9) (2020) 615-618
DOI: 10.22060/mej.2019.15136.6036

Effect of the Phase Change on the Flow Distribution in the Manifold of Fuel Cell Stack

A. Rezaei Sangtabi[1], A. Kianifar[1]*, E. Alizadeh[2], M. Rahimi[2], S. H. Masrori Saadat[2]

[1] Department of Mechanical Engineering, Ferdowsi University of Mashhad, Mashhad, Iran
[2] Fuel Cell Technology Research Laboratory, Malek Ashtar University of Technology, Feridonkenar, Iran

ABSTRACT: In this paper, the effect of water vapor phase change on the distribution of oxygen flow in the cathode side of a polymer electrolyte membrane fuel cell stack with 26 cells is investigated by using computational fluid dynamics. For this purpose, a code is developed in OpenFOAM software and validated with experimental data for the single-phase flow distribution. Three different boundary conditions are applied to the walls of the manifold: constant temperature, free and forced heat convection. The results indicate that water generated from condensation on the lower wall of the inlet manifold enters the first cell. Also, the accumulation of water in this area reduces the flow velocity at the entrance of the first cell. The condensed water vapor on the upper wall of the inlet manifold moves to the end of the stack. Part of the water enters into the last four cells, and the other part returns to the manifold due to the vortex. Therefore, the first cell and the last four cells receive less reactant than other cells. The non-uniform flow distribution parameter increases by up to 1425% on using saturated oxygen and under the forced convection condition.

Review History:

Received: 15 Oct. 2018
Revised: 16 Dec. 2018
Accepted: 11 Mar. 2019
Available Online: 10 Apr. 2019

Keywords:

Two-phase flow
Phase change
Fuel cell stack
Flow distribution
Volume fraction

1- Introduction

A single Proton Exchange Membrane Fuel Cell (PEMFC) has a potential of 0.6-1.0 V depending on the load, therefore several individual fuel cells are serially connected to create a PEM fuel cell stack [1]. The manifold system is used to feed reactant gases (fuel and oxidant) to each individual cell. Since all cells in a stack are thermally and electrically connected in series, the overall performance of a stack depends on the satisfactory operation of all individual cells [2]. It is essential that the reactants are uniformly distributed from the inlet manifold to the individual cells. Gas flow maldistribution from cell to cell could introduce water flooding, membrane drying, localized hot spots in the membrane, material degradation, which has a significant impact on the fuel cell efficiency. The flow maldistribution in the PEMFC stack has been studied using numerical and experimental approaches [3-4]. Due to the lack of experimental techniques to measure the instantaneous flow distribution, experiments of flow maldistribution reported for stack level are rarely found. Two-phase flow, turbulence, heat transfer, and variation of fluid properties were neglected in the most numerical methods. In a PEMFC, the proton conductivity of the membrane depends on its water content and using saturated reactants can improve the performance of the fuel cell. The heat transfer between saturated reactants and the walls causes condensation of part of the water vapor in the inlet gas. In this paper, the effect of the water vapor phase change on the flow distribution in the PEMFC stack is investigated at the different operating conditions.

2- Governing Equations

The unsteady laminar flow and conservative form of the two-dimensional governing equations, including that for continuity, momentum, energy, species and volume fraction in Cartesian coordinate are given as the follows [5]:

$$\frac{\partial \rho}{\partial t} + \nabla.\left(\rho U\right) = 0 \tag{1}$$

$$\frac{\partial \left(\rho U\right)}{\partial t} + \nabla.(\rho UU) = -\nabla P + \rho g + \nabla.(\mu(\nabla U + (\nabla U)^T) + F \tag{2}$$

$$\frac{\partial \left(\rho C_p T\right)}{\partial t} + \nabla.(\rho C_p UT) = \nabla.(K\nabla T) + \dot{m}H_{fg} \tag{3}$$

$$\frac{\partial (\rho y_i)}{\partial t} + \nabla.(\rho U y_i) = \nabla.(\rho D_i \nabla y_i) - \dot{m} \tag{4}$$

$$\frac{\partial \alpha_1}{\partial t} + \nabla.(U\alpha_1) + \nabla.(U_r \alpha_1(1-\alpha_1)) = -\dot{m}\left(\frac{1}{\rho_1} - \alpha_1\left(\frac{1}{\rho_1} - \frac{1}{\rho_2}\right)\right) \tag{5}$$

*Corresponding author's email: a-kiani@um.ac.ir

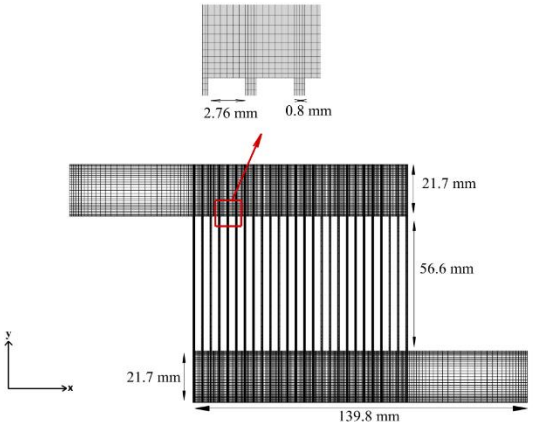

Fig. 1. Computational domain

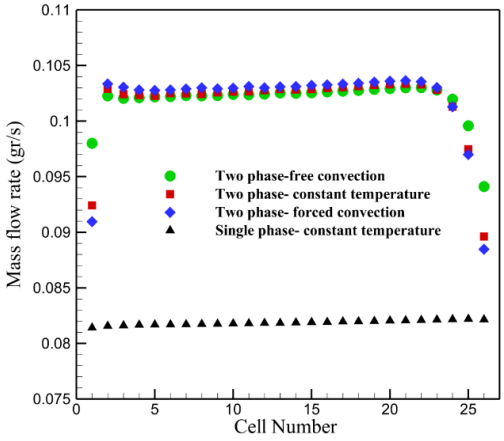

Fig. 3. Gas mass flow rate at the center of cells

Table 1. Operating parameters

Parameter	Value
Cell temperature (K)	338
Ambient temperature (K)	298
Operating pressure (Pa)	101325
Inlet humidity	100%
Oxygen mass flow rate (gr/s)	2.267

Table 2. The non-uniform flow distribution parameter

Boundary condition	F_1
pure oxygen (no phase change)	0.0096
Constant temperature	0.1329
Forced convection	0.0864
Free convection	0.1464

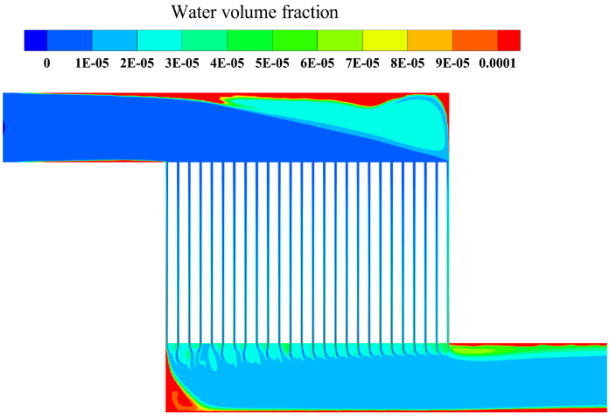

Fig. 2. Contours of liquid water volume fraction

Relevant properties, such as density, thermal conductivity, heat capacity, and viscosity are calculated by volume fraction weighted averaging:

$$\phi = \phi_1\alpha_1 + \phi_2\alpha_2 \tag{6}$$

The non-equilibrium phase changes rates are expressed as [6]:

$$\dot{m} = \begin{cases} k_{cond}(1-\alpha_1)\dfrac{M_g^{H_2O}}{\bar{R}T}P(x_g^{H_2O} - x_{sat}^{H_2O}) & x_g^{H_2O} \geq x_{sat}^{H_2O} \\ k_{evap}\alpha_1\rho_1 P(x_g^{H_2O} - x_{sat}^{H_2O}) & x_g^{H_2O} < x_{sat}^{H_2O} \end{cases} \tag{7}$$

The saturation pressure of water vapor and the latent heat of the water as a function of local temperature can be obtained using the following expression [6]:

$$P_{sat} = -2846.4 + 411.24(T - 273.15) - 10.554(T - 273.15)^2 + 0.166636(T - 273.15)^3 \tag{8}$$

$$H_{fg} = 307090(647.15 - T)^{0.35549} \tag{9}$$

3- Numerical Method and Boundary Conditions

A Two-Dimensional (2D) schematic of the simulated stack is displayed in Fig. 1. The geometry consists of the inlet and outlet manifolds and 26 cells. The dimensions for the geometry are shown in Fig. 1.

A no-slip boundary condition was applied to all solid walls. A velocity inlet boundary condition was assumed at the inlet. A zero-gauge pressure was used at the outlet. Three thermal boundary conditions were applied to the stack outer walls: constant temperature, free and forced heat convection. The governing equations were solved using the finite volume

software OpenFOAM. The pressure-velocity coupling was accomplished by the PISO algorithm. The central differencing and Euler schemes are used to discrete spatial and temporal terms.

The operating parameters used in the simulation are shown in Table 1.

4- Results

Due to the temperature difference between the inlet flow and environment, the temperature of the mixture and the saturation pressure of water vapor decreased. As the mixture cooled down, water vapor condensed to the liquid water. The contour of the volume fraction of liquid water is shown in Fig. 2.

Condensed water at the lower wall of manifold entered the first cell. The liquid water at the upper wall moved to the end of the manifold. As seen in Fig. 2, a vortex formed at the end of the manifold of the stack and returned part of the liquid water to the manifold. The mass flow rate of the gas mixture at the center of cells is calculated and is shown in Fig. 3. The first cell and the last four cells receive less reactant than other cells.

The non-uniform flow distribution parameter is used to measure the flow maldistribution [7]:

$$F_1 = \frac{\max(\dot{m}_1 ... \dot{m}_n) - \min(\dot{m}_1 ... \dot{m}_n)}{\max(\dot{m}_1 ... \dot{m}_n)} \quad (10)$$

The non-uniform flow distribution parameter for different boundary conditions is listed in Table 2. This parameter increases by up to 1425% under forced convection condition.

5- Conclusions

In this paper, the effect of phase change of water vapor on the flow maldistribution in the manifold of the fuel cell stack is investigated. The results show that the non-uniform flow distribution parameter increases by up to 1425% on using saturated oxygen and under forced convection condition.

References

[1] F. Barbir, PEM Fuel Cells, Academic Press, Boston, 2013

[2] J. Lebæk, M. Bang, S.K. Kær, Flow and Pressure Distribution in Fuel Cell Manifolds, Journal of Fuel Cell Science and Technology, 7(6) (2010) 061001-061008.

[3] S.Y. Kim, W.N. Kim, Effect of cathode inlet manifold configuration on performance of 10-cell proton-exchange membrane fuel cell, Journal of Power Sources, 166(2) (2007) 430-434.

[4] M. Sajid Hossain, B. Shabani, C.P. Cheung, Enhanced gas flow uniformity across parallel channel cathode flow field of Proton Exchange Membrane fuel cells, International Journal of Hydrogen Energy, 42(8) (2017) 5272-5283.

[5] N. Samkhaniani, M.R. Ansari, Numerical simulation of bubble condensation using CF-VOF, Progress in Nuclear Energy, 89 (2016) 120-131.

[6] P.K. Jithesh, A.S. Bansode, T. Sundararajan, S.K. Das, The effect of flow distributors on the liquid water distribution and performance of a PEM fuel cell, International Journal of Hydrogen Energy, 37(22) (2012) 17158-17171.

[7] J.M. Jackson, M.L. Hupert, S.A. Soper, Discrete geometry optimization for reducing flow non-uniformity, asymmetry, and parasitic minor loss pressure drops in Z-type configurations of fuel cells, Journal of Power Sources, 269 (2014) 274-283.